A novel diimine two-tetradentate ionic macrocycle Schiff base ligand as a Colorimetric Chemosensor for the Detection of Fe 2+ andFe 3+ ions

Mahrokh Razzaghi kamroudi
Damghan University
Gholamhossein Grivani
grivani@du.ac.ir

Damghan University

Research Article

Keywords: Two-tetradentate, Ionic macrocycle Schiff base ligand, Metal ions, Colorimetric, Chemosensor, Detection

Posted Date: November 25th, 2024

DOI: https://doi.org/10.21203/rs.3.rs-5400352/v1

Additional Declarations: No competing interests reported.

A novel diimine two-tetradentate ionic macrocycle Schiff base ligand as a Colorimetric Chemosensor for the Detection of Fe^{2+} and Fe^{3+} ions

Mahrokh Razzaghi kamroudi[1], Gholamhossein Grivani[1*]

[1] School of Chemistry, Damghan University, Damghan, P. O. Box, 36715-364, Iran

[*] Corresponding author. E-mail: grivani@du.ac.ir

Abstract

In this paper, a novel diimine two-tetradentate ionic macrocycle Schiff base ligand (L) was synthesized by reacting 1,2-bis((1H-imidazol-1-yl)methyl)benzene (OB) with 5- chloromethyl salicylaldehyde in methanol and followed by the addition of ethylenediamine under refluxing conditions, and characterized by elemental analysis, FT-IR, UV–Visible, fluorescence, proton nuclear magnetic resonance (^{1}H NMR), carbon-13 nuclear magnetic resonance (^{13}C NMR), liquid chromatography coupled to tandem mass spectrometry (LC-MS/MS). The sensing ability toward the metal ions of Mo^5+, V^{4+}, Cr^{3+}, Al^{3+}, Zn^{2+}, Cd^{2+}, Hg^{2+}, Cu^{2+}, Ni^{2+}, Co^{2+}, Mn^{2+}, Sn^{2+}, Pb^{2+}, Fe^{3+}, Fe^{2+}, K^+, Ag^+, Mg^{2+}, Ca^{2+}, Ba^{2+} and Na^+ was investigated in mixture of dimethyl sulfoxide (DMSO) and water (H_2O) (2/8, v/v) solvent. The L is used as a colorimetric chemosensor for the detection of Fe^{2+} and Fe^{3+} ions, by a rapid and significant color change from yellow to brown and brownish red Respectively, by the naked eye and at room temperature. Also, the limit of detection (LOD) was obtained 0.45 µM for Fe^{2+} and 0.68 µM for Fe^{3+}. Job's plots indicated a 1:2 complexation stoichiometry between the sensor (L) and Fe ions. Moreover, the sensor (L) demonstrated reversible behavior upon the addition of EDTA. This probe (L) could be prepared into test paper strips for visual detection of Fe^{2+} and Fe^{3+} ions at room temperature.

Keywords Two-tetradentate, Ionic macrocycle Schiff base ligand, Metal ions, Colorimetric, Chemosensor, Detection

1 Introduction

Schiff bases are a class of organic compounds characterized by an imine (-C=N) functional group formed by simple reaction of the primary amines and the aldehydes or ketones [1]. Schiff base ligands have been extensively studied in coordination chemistry mainly due to their facile syntheses, easily tunable steric, electronic properties and good solubility in common solvents. Synthesized Schiff bases used as antibacterial [2], antifungal [3], anti-inflammatory [4], analgesic [5], anticancer [6] and corrosion inhibition [7]. In industry, they are used as antioxidant agents [8], colorimetric fluorescent sensors and as primary compound to synthesis of new compounds [9]. Schiff base derived from an aromatic aldehyde and aromatic amine is more stable because of having effective conjugation and readily synthesizing. Due to the presence of the imine group, Schiff base compounds can act as ligands, forming transition metal Schiff base complexes [10–12]. These complexes often exhibit valuable properties, such as catalytic activity, fluorescence, and magnetic behavior. Thus, from last few decades Schiff bases have been drawing attention of the researchers in coordination chemistry, due to their capability of forming stable complexes with metal ions and also, for their high selectivity and sensitivity towards specific metal ions [13–15]. Selective sensing and monitoring of transition metal ions is highly important since these metal ions have a strong influence on chemical, biological, and environmental process [16–20]. Several approaches including electrochemical, atomic absorption, and chromatographic methods have been explored [21–23]. Among the organic molecules, Schiff bases have promising optical response towards metal ions because of their high chelating ability. Their donor–acceptor ease with different metal ions provides efficient use in metal ion detection.

[*] Corresponding author. E-mail: grivani@du.ac.ir

The chemical interactions between Schiff bases and metal ions are critical for generating sensing signals [24]. In the case of Schiff base chemo-sensors, the change in their electronic properties via different charge transfer processes (e.g., ligand-to-metal charge transfer and/or metal-to-ligand charge transfer) produces the sensing signal. Thus they have been primarily explored as optical metal ion sensors. The signals of these sensors exhibited strong dependency upon the interactions between metal ions and Schiff bases. The development of synthetic receptors for the detection and sensing of anions and cations is an emerging research area in the field of donor–acceptor chemistry [7,19,22,25]. Many Schiff base ligands have been used as chemosensors for various metal ions such as Zn^{2+} [18], Hg^{2+} [22,26], Cu^{2+} [27], Fe^{3+} [28], and Cr^{3+} [24]. In recent years, supramolecular chemistry has emerged as one of the actively pursued research fields of the chemical sciences [29]. Schiff base imine condensations are a useful tool for macrocycle synthesis and applications within supramolecular chemistry [30].

Macrocyclic molecules often serve as receptors in supramolecular chemistry. Advantages of the macrocyclic approach include: control of nuclearity and solubility, enhanced thermodynamic stability (macrocyclic effect), and the ability to fine-tune the metal ion environment and stabilize redox products. It is well established that the degree of unsaturation and the size of the macrocycle have a pronounced effect on the relative stability of the various oxidation states available to the encapsulated transition metal ion. The more rigid structure of macrocycles than their acyclic analogues helps to control and maintain the geometry of their binding site, and makes them more selective [30,31]. As a result, significant effort is being put into building viable sensors capable of detecting and evaluating transition metal ions, and anions in biological systems to detect serious human illness. Iron is one of the most essential trace elements in biological systems, and it plays a major role in the function of hemoglobin and various enzymes in the human body. It is also crucial for cellular metabolism and is widely present in the environment. Iron deficiencies and overloads can lead to serious disorders, including Huntington's disease. Any imbalance between Fe^{2+} and Fe^{3+} in nature can result in a range of health issues such as anemia, liver and kidney damage, diabetes, and heart disease [17,19,32]. High levels of Fe^{2+} in water can stimulate the growth of specific algae species, reduce oxygen levels, cause water turbidity, and create dead zones, which can harm other aquatic organisms and ecosystems. In humans, excessive Fe^{2+} in drinking water can cause iron overload, known as hemochromatosis, leading to organ damage, particularly in the liver, heart, and pancreas, as well as gastrointestinal distress, joint pain, and fatigue. On the other hand, excessive exposure to Fe^{3+} in humans can disrupt the iron balance in the body, affecting the absorption, utilization, and storage of iron, which can lead to iron overload or deficiency with various negative health consequences. Particularly, molecular chemosensors that show optical (both colorimetric and fluorescence) responses upon selective binding with target metal ions have received great interest due to their advantages such as being cost-effective, rapid, real-time-monitoring, and naked-eye detectable [7,33].

In this research, it is described the synthesis of a diimine two-tetradentate ionic macrocycle Schiff base ligand assigned as L (Scheme 1) and used it as chemosensor for detection of Fe^{2+} and Fe^{3+} ions.

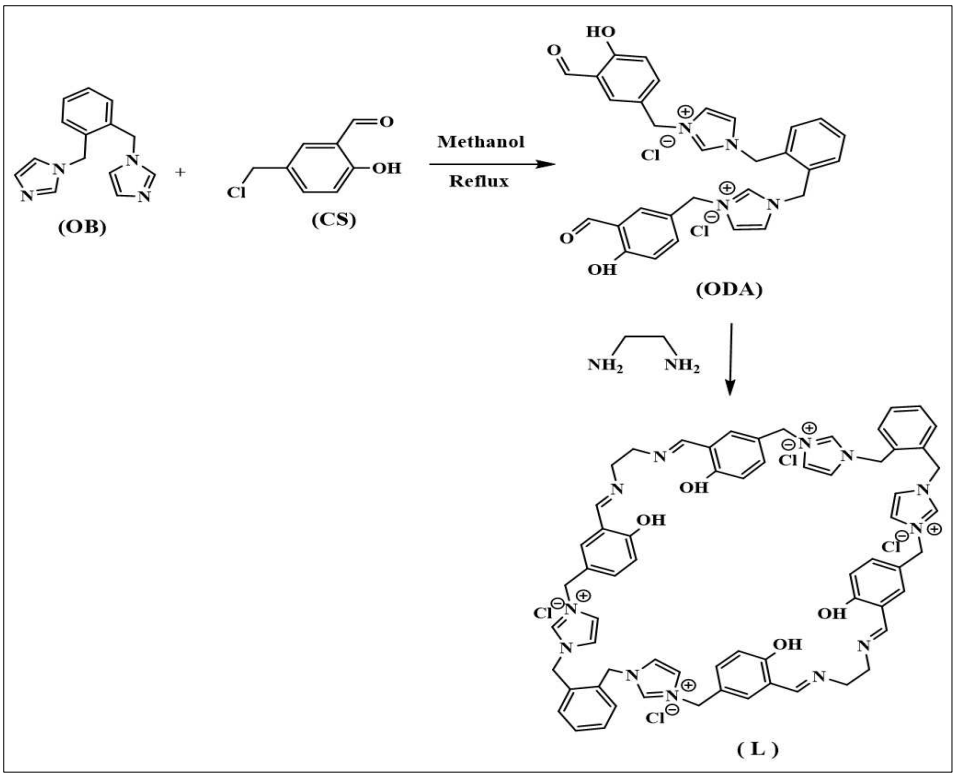

Scheme 1 Synthetic procedures of L.

2 Experimental

2.1 Materials and methods

5-Chloromethyl salicylaldehyde (CS) (99%) was prepared following the method reported in the literature [34]. All solvents and reagents were commercially available from Aldrich and Merck and used without further purification for synthesis and/or analyses. Elemental analysis (C, N, and H) was recorded on a CHNS-932 (Heraeus) elemental analyzer. The FT-IR (Fourier transform infrared) spectrum (4000-400 cm^{-1}) of the compounds were recorded as KBr pellet a PerkinElmer FT-IR spectrophotometer. UV-Vis absorption spectra were recorded with a PerkinElmer Lambda 25 spectrophotometer in the 200–700 nm region. Fluorescence measurements were carried out on a Hitachi on FP 6200 fluorescence spectrophotometer. UV-Visible and fluorescence measurements were conducted in a mixture of dimethyl sulfoxide (DMSO) and water (H_2O) (2/8, v/v) at room temperature. The ^1H and ^{13}C NMR spectrum were recorded on a 400 MHz Brucker spectrometer with DMSO-d_6 was used as a solvent and tetra methylsilane (TMS) as an internal standard at 25 °C. The mass spectra of the compounds have been recorded with using the Shimadzu spectrometer (GCMS QP 1000 EX and Liquid Chromatography Tandem Mass spectrometer (LC-MS/MS) on a Shimadzu UFLC-AB Sciex 3200 QTRAP. Melting points (°C) of compounds were determined on the BI Barnstead electrothermal instrument.

2.2 Synthesis of 1,2-bis((1H-imidazol-1-yl)methyl)benzene (OB)

This compound was prepared by the preparation method described in reference [35]. In a 100 mL round bottom flask, α,α'-Diboromo-o-xylene (1.17 g, 4.43 mmol) was added to a solution of imidazole powder (3.16 g, 46.4 mmol) in 50 mL of absolute methanol. The mixture was refluxed for 18 hours with continuous stirring. After cooling to room temperature, K_2CO_3 (6.13 g) was added to the colorless solution, and the reaction mixture was left at room temperature for 2 hours. The white crystals were filtered off and washed three times with a 1:1 mixture of methanol and water (10 mL each). The crystals were then dried in air for one day. The final product had a white color. Yield: 0.69 g (57%). M. p: 102-103 °C. Chemical Formula: $C_{14}H_{14}N_4$. IR spectrum (KBr, cm^{-1}): 3115-2900 cm^{-1} (aliphatic and aromatic C-H str), 1627 cm^{-1} (C=N imidazole ring str), 1530-1440 cm^{-1} (C=C, benzene and imidazole ring str), 1349 cm^{-1} (C-N bend). ^1H NMR (400 MHz, in DMSO-d_6, d, ppm): 7.71 (2Ha, a' protons of

imidazole rings), 7.29-6.93 (6Hb,b',c,c',d,d' protons of benzene and imidazole rings), 5.31 (2He,e' protons of imidazole rings), 3.48 (2Hf,f' protons of methylene groups). ^{13}C NMR (100.53 MHz, DMSO-d_6, d, ppm): 137.7 (C1,1'), 135.2 (C2,2'),128.8 (C3,3'), 128.3 (C4,4'), 128 (C5,5'), 119.8 (C6,6'), 46.3 (C7,C7') ppm. Mass (m/z): 238 (Mw), 236, 163, 142, 90, 28.

2.3 Synthesis of ODA

To synthesize of the ODA, 0.238 g (1 mmol) of OB was dissolved in 20 ml of acetonitrile and mixed with 0.341 g (2 mmol) of compound CS dissolved in 20 ml of acetonitrile in a 100 mL flask. The mixture was heated under reflux conditions for 8 hours with stirring, resulting in the formation of a clear yellow solution and then the solvent was evaporated using a rotary evaporator. Then, it was washed three times with a solution of ethanol and ether in a 1:1 molar ratio and then dried at room temperature. Color: Light Yeld: 0.78 g (80%). M. p: 110-112 °C. Chemical Formula: $C_{30}H_{28}Cl_2N_4O_4$. Anal. Calcd for (ODA) (%): C: 62.18, H: 4.87, N: 9.67. Found (%): C: 60.30, H: 5.07, N: 9.38. IR spectrum (KBr, cm^{-1}): ν(O—H), 3424; ν(C—H)aromatic, 3112-3056; ν(C—;H)aliphatic, 2874; ν(C—H)aldehyde, 2556; ν(C═O), 1654; ν(C═C), 1488–1448; ν(C—O),1150. ^{1}H NMR (δ, ppm; DMSO-d_6): 10.28-10.25 (2H, Haa'); 9.31-9.28 (2H, b,b' protons of aldehyde); 7.44-6.88 (protons of benzene and imidazole rings); 5.50-5.15 (4H, Hl,l',k,k' methylene protons of ethylene diamine groups). ^{13}C NMR (100.53 MHz, DMSO-d_6, δ, ppm): 191.3 (C1,1' aldehyde carbons), 159.9-155.6 (C2,2' phenolic group carbons), 138.5-98.8 (carbons of imidazole and benzene), 53.4-49 (C14,14',15,15' methylene groups). Mass (m/z): 579 (Mw), 507, 370, 222, 130, 97, 58.

2.4 Synthesis of probe L

In a 500 ml two necks round bottom Flask, containing 250 ml methanol and ODA (0.96 g, 1.6 mmol,) was added the solution of ethylenediamine (0.10 g, 1.6 mmol in 100 ml methanol) during 5h in reflux conditions, and the content was refluxed for 2 h else. The solvent was evaporated and the yellow precipitates were washed three times with ethanol and ether and the obtained Schiff base macrocycle (L) was dried in air for 1 day. Color: yellow. Yield: 1.6 g (83 %). M. p: >300 ◦C. Chemical Formula: $[C_{64}H_{64}Cl_4N_{12}O_4]$. Anal. Calcd (%): C: 63.68, H: 5.34, N: 13.92. Found (%): C: 62.75, H: 5.43, N: 13.73. IR spectrum (KBr, cm^{-1}): 3433 ν(O—H) phenolic, 3166 ν(C—H) aromatic, 2902 ν(C—H) aliphatic, 2364 ν(C—H) iminic, 1636 ν(C═N), 1497-1458 ν(C═C), 1149 ν(C—O). ^{1}H NMR (δ, ppm; DMSO-d_6): 13.63 (s, 2Hc,c' (phenolic protons)), 9.24-9.17 (s, 2Hb,b' (azomethine protons)), 9.14-6.81 (m, Hd,d',j,j',I,I',h,h',l,l',m,m',e,e',f,f' (protons of benzene and imidazole rings)), 5.53-5.33 and 4.33-3.94 ((4Hg,g') and (4Hk,k') (methylene protons)), 3.52-2.48 (4Ha,a' (methylene protons of ethylene diamine groups)). ^{13}C NMR (100.53 MHz, DMSO-d_6, δ, ppm): 166.9-161.4 (C4,4' (phenolic carbons)),137.5, 136.2 (C2,2' (azomethine carbons)), 136, 133, 132.8, 132.3, 131.9, 129.7, 128.8, 128.5, 128.4, 128.3, 128.2, 123, 122.7, 120, 119.7, 118.5, 116.4 (C10,10',3,3',5,5',6,6',7,7',8,8',11,11',12,12'), 73.11-57.2 (C9,9' (methylene carbons)), 53.5-46.7 (C13,13' (methylene carbons)), 31-25.1 (C1,1' (ethylene diamine carbons)). LC-MS/MS (m/z): 1207 (Mw), 1110, 1098, 1064, 931, 764, 561, 413, 305, 292, 171, 117. UV-Vis (DMSO: H_2O (2/8, v/v)): ((λ_{max} (nm), (ε, (L Mol^{-1} cm^{-1})): 259 and 316, $22 \times 10^{+3}$ and $9 \times 10^{+3}$.

3 Result and discussion

3.1 Synthesis and characterization of the L

The macrocycle L was synthesized by the reaction of compounds ODA and ethylene diamine in methanol solvent under reflux conditions. After evaporation of the solvent, the macrocycle ionic-Schiff base ligand was obtained as a yellow precipitate. The new ligand (L) was characterized by numerous methods, including elemental analysis, ^{1}H NMR, ^{13}C NMR, FT-IR, UV-Vis and spectroscopies and LC-MS/MS spectrometer.

3.2 CHN analysis and FT-IR spectra

The data from elemental analysis and physical attributes of the synthesized compounds are summarized in Table 1. The correspondences of experimental and theoretical amount of C, H and N content confirm the chemical composition of related compounds.

Table 1 Physical attributes and analytical data of the synthesized compounds.

Compound	Molecular formula	Color	Yield (%)	Melting Point (°C)	Elemental analysis (%) found (calculate)		
					C	H	N
OB	$[C_{14}H_{14}N_4]$	white	57	102-103	70.39 (70.57)	6.19 (5.92)	23.42 (23.51)
ODA	$[C_{30}H_{28}Cl_2N_4O_4]$	Light Yellow	80	110-112	62.05 (62.18)	5.07 (4.87)	9.38 (9.67)
L	$[C_{64}H_{64}Cl_4N_{12}O_4]$	Yellow	83	>300	63.75 (63.68)	5.43 (5.34)	13.73 (13.92)

The FT-IR spectra of compounds were recorded in the range of 400-4000 cm^{-1} at room temperature. The macrocycle Schiff base ligand (L) exhibits a broad absorption band centered on 3433 cm^{-1} that can be assigned to O–H stretching arising from the presence of the phenolic group and the strong band observed in the 1636 cm^{-1} was assigned to the azomethine group vibration. The hydrocarbon part of this ligand was evidenced by the presence of aromatic and aliphatic C-H wave numbers at aria of 3166 cm^{-1} and 2902 cm^{-1}, respectively. In addition, the FT-IR spectrum of L displayed stretching bands at 1497-1458 cm^{-1}, and 1149 cm^{-1}, which are assigned to ν(C═C), and phenolic ν(C-O), respectively. These data generally confirm the suggested coordination site and identify the main groups of the synthesized macrocycle Schiff base ligand [36].

3.3 ^{1}H / ^{13}C NMR spectroscopy

The ^{1}H and ^{13}C NMR spectra were recorded in DMSO-d_6 (Figs.1 and 2). The signals in ^{1}H NMR spectrum of L as singlet at 13.63 ppm was correspond to the phenolic OH groups (Hc,c') and the signals at the 9.24-9.17 ppm corresponded to the iminic protons. The corresponding signals of the methylene protons (g,g') and (k,k') are observed in the region 5.53-5.33 and 4.33-3.94 ppm, respectively, and the methylene protons of ethylene diamine are observed at 3.58 and 2.48 ppm. In addition, the chemical shifts due to aromatic protons are located as multiplet (d,d',j,j',I,I',h,h',l,l',m,m',e,e',f,f') at 9.14-6.81 ppm. The ^{13}C NMR spectrum of the L (Fig. 2) shows phenolic carbon (4,4') and azomethine carbon (2,2') signals at region 166.9-161.4 ppm and 137.5 -136.2 ppm, respectively. The imidazolium and phenyl ring carbons (C10,10',3,3',5,5',6,6',7,7',8,8',11,11',12,12') of L resonate at region 136, 133, 132.8, 132.3, 131.9, 129.7, 128.8, 128.5, 128.4, 128.3, 128.2, 123, 122.7, 120, 119.7, 118.5, 116.4 ppm. The signals, displayed in the regions 73.11-57.2 ppm and 53.5-46.7 ppm can be related to resonances of the methylene of salicylate (9, 9') and xylene (13, 13') moieties, respectively. Eventually, the carbons of methylene of ethylene diamine functionalities (1, 1') were assigned, as signals at the region of 31-25.1 ppm. Thus, these NMR data confirm the functionalities and the structure of the ionic macrocycle Schiff base compound of L [37].

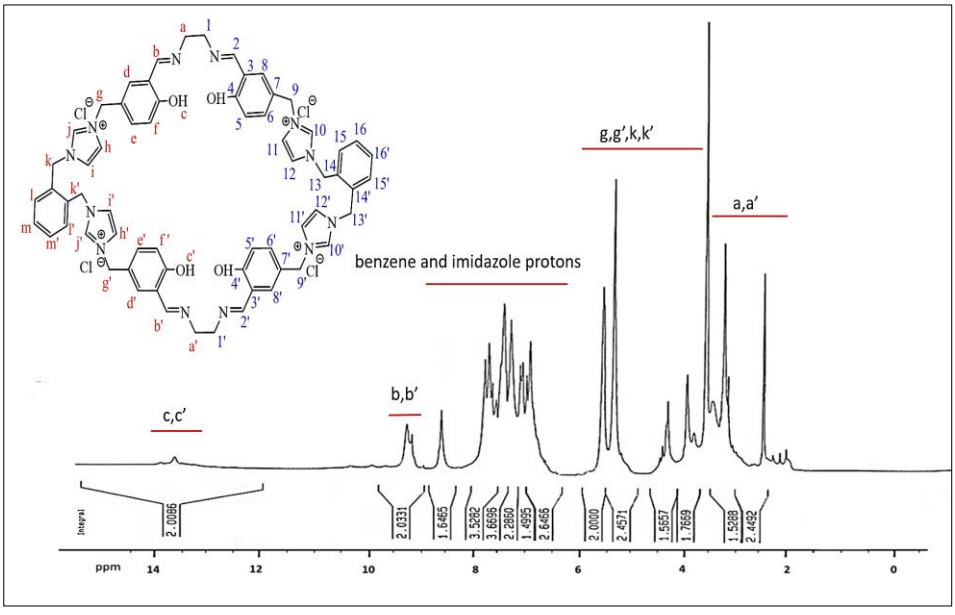

Fig. 1 ^{1}H NMR spectrum of L in DMSO-d_6.

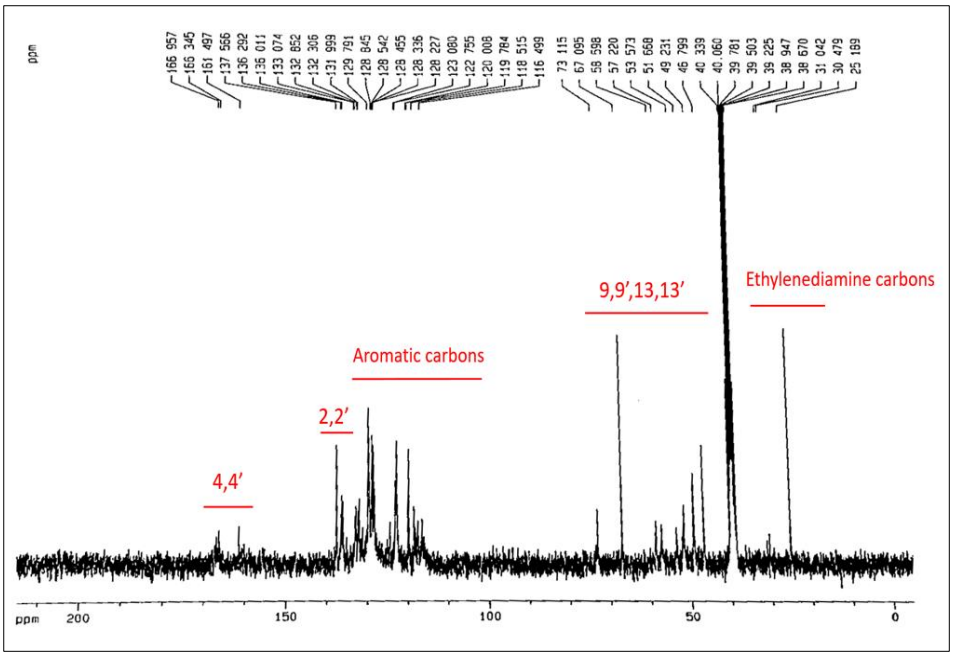

Fig. 2 ^{13}C NMR spectrum of L in DMSO-d_6.

3.4 LC-MS/MS spectrometry

The Mass spectrometry of the L can be easily explained based on the Liquid Chromatography Tandem Mass spectrometer (LC-MS/MS) (Fig. 3). LC-MS/MS spectrometry analysis of L shows an isotope pattern at m/z = 1207 was in agreement with the formula weight of the ligand ($C_{64}H_{64}Cl_4N_{12}O_4$) with molecular weight 1207 g/mol. "Isotopic pattern" is an important aspect observed in LC-MS/MS spectra, especially for compounds containing elements with multiple stable isotopes. This pattern appears as distinct m/z peaks corresponding to different isotopic compositions of a given compound or its fragments. The presence of multiple isotopes causes changes in the intensity and position of the peaks in the LC-MS/MS spectrum of the macrocyclic ligand displays specific m/z values for different fragments. The analysis of these fragments helps in the identification, characterization, and molecular weight of the molecule. Some fragments accompanied by related m/z values are given as 1207 ($C_{64}H_{64}Cl_4N_{12}O_4$), 1110 ($C_{63}H_{57}Cl_4N_{11}$), 1098 ($C_{62}H_{57}Cl_4N_{11}$), 1064 ($C_{60}H_{48}Cl_4N_{11}$), 931 ($C_{51}H_{36}Cl_4N_{10}$), 764 ($C_{40}H_{29}Cl_4N_8$), 561 ($C_{28}H_{13}Cl_4N_5$), 413 ($C_{28}H_7N_5$), 305 ($C_{20}H_9N_4$), 292 ($C_{19}H_8N_4$), 239 ($C_{15}H_6N_4$), 171 ($C_{11}H_9N_2$), 117 ($C_3H_4N$), the structures of the theme are given in Supplementary information (Table S1). Thus, all the analysis and spectral data are in good agreement with the proposed structure of the synthesized ligand [38].

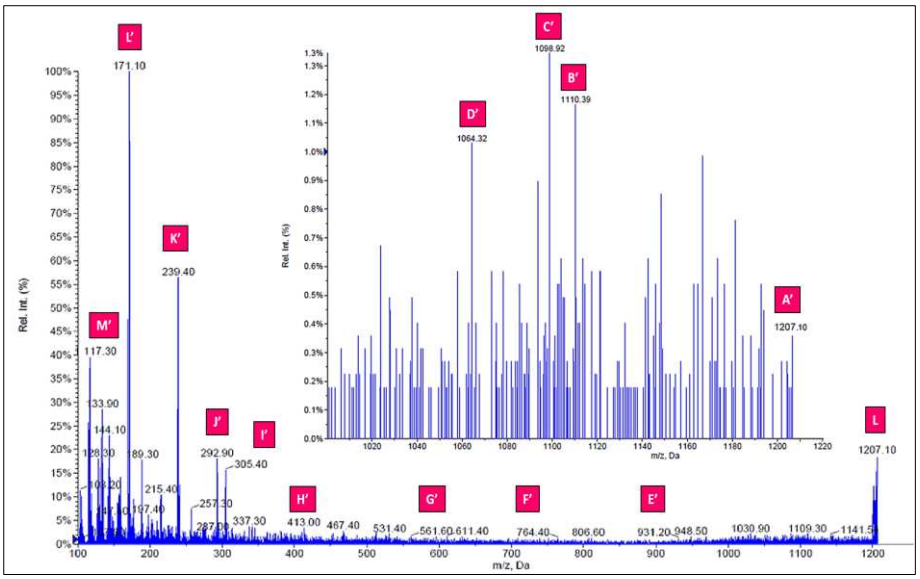

Fig. 3 LC-MS/MS spectrum of L.

3.5 UV-Vis Spectral Studies

The UV-Vis spectrum of the L is displayed in Fig. 4. There are two absorption peaks for L, in the wavelength range of 253–653 nm in DMSO: H_2O (2/8, v/v) (5×10^{-5} M) at room temperature. The strong absorption with a λ_{max} at 259 nm ($\varepsilon = 22 \times 10^{+3}$ L Mol^{-1} cm^{-1}) is related to π-π^* transitions of aromatic rings and imine groups. In addition, the absorption band with a λ_{max} of 316 nm ($\varepsilon = 9 \times 10^{+3}$ L Mol^{-1} cm^{-1}) is attributed to n-π^* transitions [36].

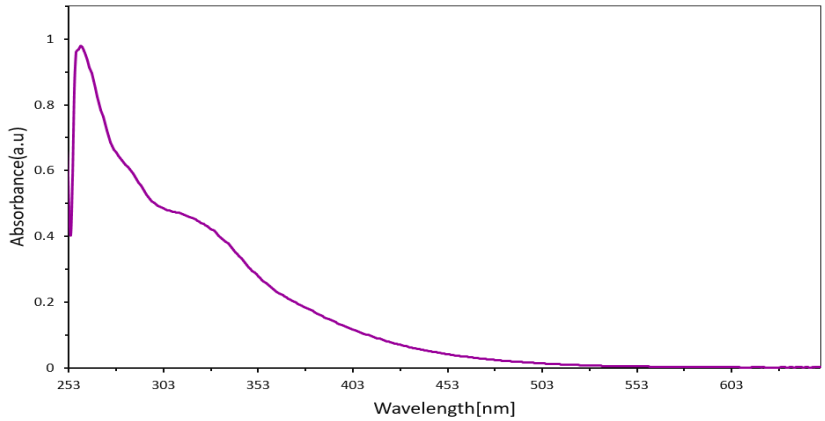

Fig. 4 UV-Vis spectra of macrocycle ionic Schiff base ligand (L) in DMSO: H_2O (2/8, v/v) solution at room temperature.

3.6 Ion-selective detection studies by L (Selectivity, sensitivity, and effect of other cations)

3.6.1 Investigating the colorimetric properties of the macrocycle ionic Schiff base ligand (L) in the presence of various metal cations with the naked eye sensing)

To study the colorimetric sensing ability of L by different metal ions, by addition equimolar of various metal ions in separately solution (5×10^{-5} M) such as Mo^{5+}, V^{4+}, Cr^{3+}, Al^{3+}, Zn^{2+}, Cd^{2+}, Hg^{2+}, Cu^{2+}, Ni^{2+}, Co^{2+}, Mn^{2+}, Sn^{2+}, Pb^{2+}, Fe^{3+}, Fe^{2+}, K^+, Ag^+, Mg^{2+}, Ca^{2+}, Ba^{2+} and Na^+ to the L, in DMSO: H_2O (2/8, v/v) (5×10^{-5}M) at room

temperature and normal light, the color changes were observed and recorded. When Fe^{2+} and Fe^{3+} were added to the L solution, a rapid and significant color change occurred, changing from yellow to brown for Fe^{2+} ion and from yellow to brownish red for Fe^{3+}. Interestingly, changes in color due to the presence of different tested cations are not significant. This color change was easily seen with the naked eye in the ambient light (Fig. 5).

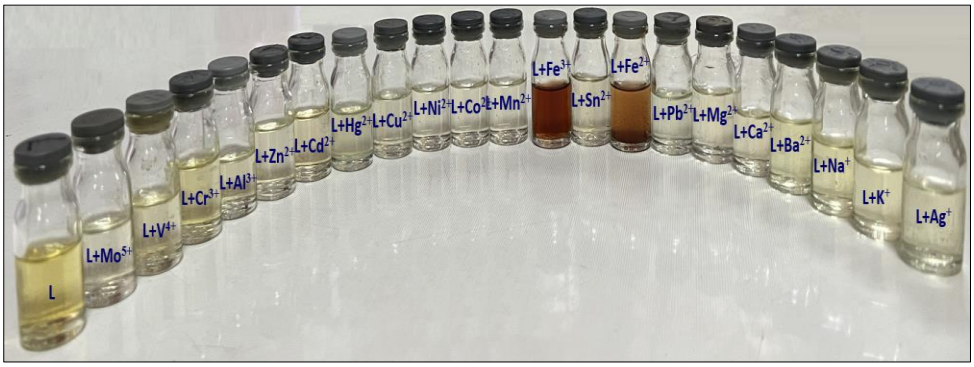

Fig. 5 The color change of solution of L in DMSO: H_2O (2/8, v/v) (5×10^{-5} M) in the presence of various cations (5×10^{-5} M) at room temperature under normal light (left to right L, Mo^{5+}, V^{4+}, Cr^{3+}, Al^{3+}, Zn^{2+}, Cd^{2+}, Hg^{2+}, Cu^{2+}, Ni^{2+}, Co^{2+}, Mn^{2+}, Fe^{3+}, Sn^{2+}, Fe^{2+}, Pb^{2+}, Mg^{2+}, Ca^{2+}, Ba^{2+}, Na^{+}, K^{+} and Ag^{+}.

3.6.2 UV-Vis studies of sensor L

UV-Vis spectrophotometer was also used to check the colorimetric properties of sensor L in the presence of different cations. Fig. 6 shows the UV-Vis spectrum of sensor L dissolved in DMSO: H_2O (2/8, v/v) (5×10^{-5} M) in the presence of various cations (Mo^{5+}, V^{4+}, Cr^{3+}, Al^{3+}, Zn^{2+}, Cd^{2+}, Hg^{2+}, Cu^{2+}, Ni^{2+}, Co^{2+}, Mn^{2+}, Sn^{2+}, Pb^{2+}, Fe^{3+}, Fe^{2+}, K^{+}, Ag^{+}, Mg^{2+}, Ca^{2+}, Ba^{2+}, Na^{+}) in a mixture of DMSO: H_2O (2/8, v/v) (5×10^{-5} M) at room temperature and in the range of 250-650 nm. As shown, in the presence of Fe^{2+} and Fe^{3+}, the UV-Vis absorption bands of sensor L undergo significant changes. However, the presence of other tested cations does not cause appreciable changes in the absorption bands of sensor L under the same conditions. In the UV-Vis spectrum of sensor L in the presence of cation Fe^{2+} three absorption bands are observed in the region of 471 nm ($\varepsilon = 8 \times 10^{+3}$ L Mol^{-1} cm^{-1}), 382 nm ($\varepsilon = 2 \times 10^{+3}$ L Mol^{-1} cm^{-1}), and 252 nm ($\varepsilon = 21 \times 10^{+3}$ L Mol^{-1} cm^{-1}). Also, four absorption bands are observed in the presence of Fe^{3+} in the region of 456 nm ($\varepsilon = 18 \times 10^{+3}$ L Mol^{-1} cm^{-1}), 361 nm ($\varepsilon = 13 \times 10^{+3}$ L Mol^{-1} cm^{-1}), 311 nm ($\varepsilon = 10 \times 10^{+3}$ L Mol^{-1} cm^{-1}) and 271 nm ($\varepsilon = 6 \times 10^{+3}$ L Mol^{-1} cm^{-1}). In the cases of Fe^{2+}, by the coordination of nitrogen and oxygen atoms to Fe^{2+} and the formation of complex, the absorption band at 251 nm, which is related to the π-π* transitions of the sensor (L), has appeared in the similar region at 250 nm .The absorption band of sensor L at 316 nm has been shifted 66 nm towards a red shift in the presence of cation Fe^{2+}. These absorption changes are ligand origin and are attributed to intra-ligand transitions, specifically π-π* and n-π*. Furthermore, in the presence of cation Fe^{2+} a new absorption band has appeared in a broad form in the region of 471 nm. This band may be related to the transitions of metal to ligand (MLCT) or ligand to metal (LMCT) transitions [7,39].

In the cases of Fe^{3+} the absorption band at 259 nm of the sensor (L), has appeared in the region 271 nm, which has shifted 12 nm towards a red shift in comparison to sensor L. In the presence of Fe^{3+}cation, the absorption band of the sensor (L) at 316 nm region has been exhibiting slight changes. In addition, a new absorption band at 361 nm was observed due to formation of complex via interaction of sensor L with Fe^{3+}. These absorption changes are of ligand origin and are attributed to intra-ligand transitions, specifically π-π* and n-π*. Furthermore, a new absorption band has appeared in a broad form at 456 nm, that could be related to the transitions of metal to ligand (MLCT) or ligand to metal (LMCT) transitions which indicates the interaction Fe^{3+} with the nitrogen and oxygen groups in sensor L, resulting in the formation of complexes [36,40]. The addition of Fe^{2+} and Fe^{3+} cations to the sensor L solution causes changes in the absorption bands of the UV-Vis spectrum and the color of their solutions. These changes indicate that the ionic macrocycle Schiff base (L) can be used for detecting Fe^{2+} and Fe^{3+} cations through colorimetry and by naked-eye observation in aqueous media.

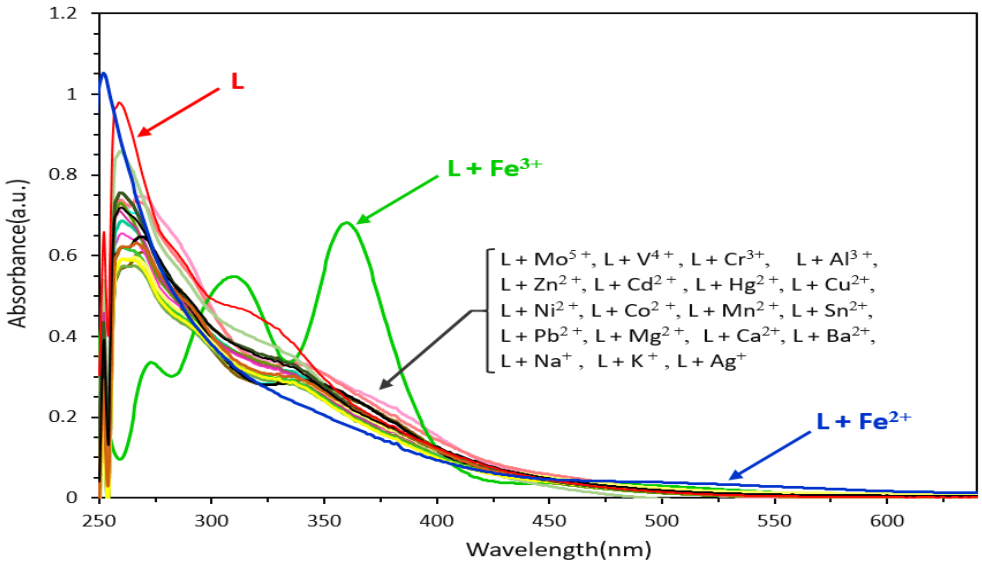

Fig. 6 UV-Vis absorption spectra of L (5×10^{-5} M) and the effect of the various cation (5×10^{-5} M) on absorption spectra of L in DMSO: H_2O (2/8, v/v) solution at room temperature.

To investigate the interference studies of the L selective sensor for Fe^{2+} and Fe^{3+} in the presence of other metal cations, it was prepared a ligand mixture solution (50 µM) with different metal cations (Mo^{5+}, V^{4+}, Cr^{3+}, Al^{3+}, Zn^{2+}, Cd^{2+}, Hg^{2+}, Cu^{2+}, Ni^{2+}, Co^{2+}, Mn^{2+}, Sn^{2+}, Pb^{2+}, Fe^{3+}, Fe^{2+}, K^{+}, Ag^{+}, Mg^{2+}, Ca^{2+}, Ba^{2+}, Na^{+}) at equimolar concentrations (50 µM) in DMSO: H_2O solution (2/8, v/v). It was done both in the presence and absence of Fe^{2+} and Fe^{3+}cations at room temperature. Afterward, it was checked for color changes and changes in absorption bands in UV-Vis spectrum in the range of 253-653 nm. As shown in Fig. 7, no significant changes were observed in the color and absorption bands of the UV-Vis spectrum when other cations were added to the solution containing Fe^{2+} or Fe^{3+} cation and sensor (L) at room temperature. These results confirm that sensor L is selective and effective sensor for detection of Fe^{2+} and Fe^{3+}cations in the presence of other metal cations.

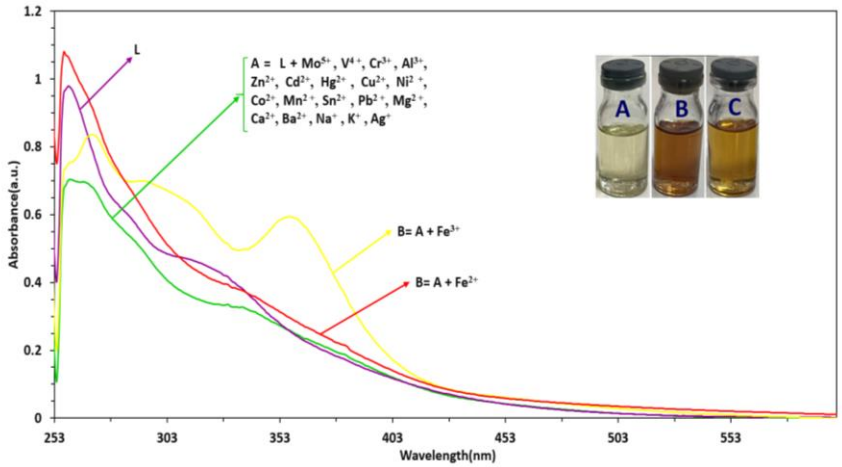

Fig. 7 Selectivity studies of L for Fe^{2+} and Fe^{3+} (50 µM) in the presence of other metal cations (50 µM).

3.6.3 UV-Vis absorbance titration of sensor L and determination of detection limit (LOD) for Fe^{2+} and Fe^{3+}

The UV-Vis spectrum titration was carried out to determine the sensitivity of L to Fe^{2+} and Fe^{3+} in DMSO: H_2O (2/8, v/v) at room temperature in the range of 250–650 nm. As shown in Figs. 8 and 9 in the UV-Vis spectra of L solutions (5×10^{-5} M) in DMSO: H_2O (2/8, v/v), an increase in the intensity of new bands at 460 nm for Fe^{2+} and 456 nm for Fe^{3+} by addition of different concentrations of Fe^{2+} and Fe^{3+} (0-10 µM). The detection limit of the sensor L for Fe^{2+} and $Fe^{3+}$was calculated from the UV-Vis titration at room temperature and calibration curves were plotted by measuring absorption intensity with different concentrations of Fe^{2+} and Fe^{3+} (0-10 µM) which showed a good linear relationship (R^2 = 0.9975, and 0.9962 for Fe^{2+} and Fe^{3+}, respectively) as depicted in Fig. 8 and Fig. 9 (inset). By using the equation LOD = 3σ/m (σ is the standard deviation and m is the slope of the intensity versus), LODs for Fe^{2+} and Fe^{3+} were determined as 0.45 µM and 0.68 µM, respectively [41].

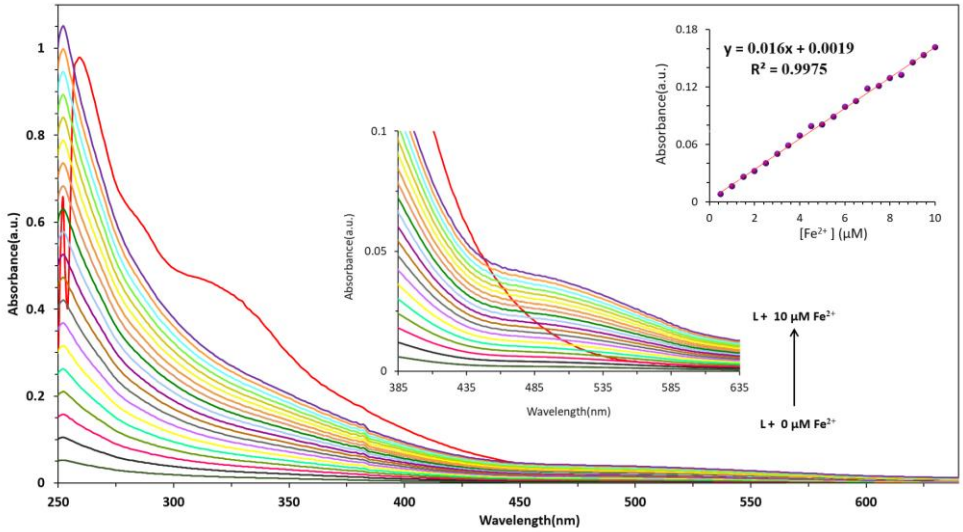

Fig. 8 UV–Vis absorption spectra of L (5×10^{-5} M) in DMSO: H_2O (2/8, v/v) solution after gradual addition of Fe^{2+} (0 - 10 µM) in DMSO: H_2O (2/8, v/v), at room temperature. Inset: plot of the linear relative absorption intensity (A) versa the concentration of Fe^{2+} within the range of 0-10 µM at λ_{max} = 460 nm.

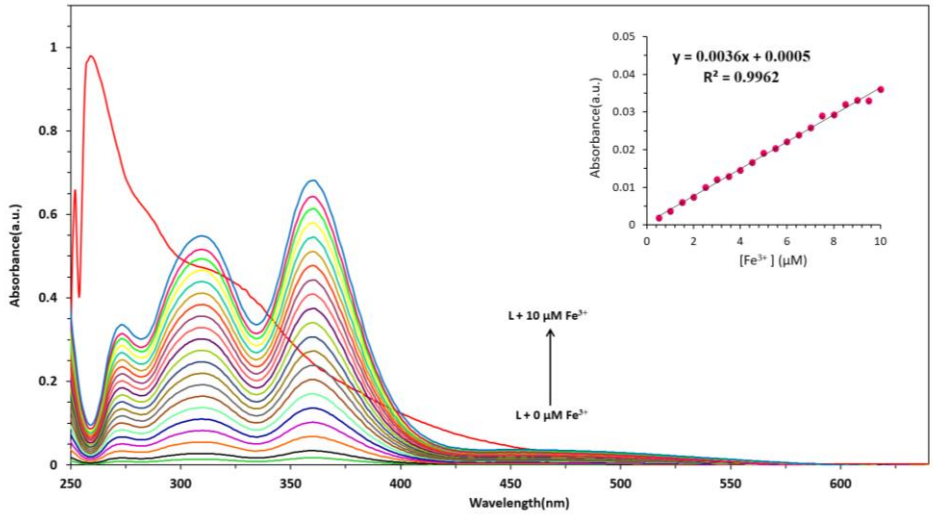

Fig. 9 UV-Vis absorption spectra of L (5×10^{-5} M) in DMSO: H_2O (2/8, v/v) solution after gradual addition of Fe^{3+} (0 - 10 µM) in DMSO: H_2O (2/8, v/v), at room temperature. Inset: plot of the linear relative absorption intensity (A) versa the concentration of Fe^{3+} within the range of 0-10 µM at λ_{max} = 456 nm.

The detection limit achieved for Fe^{3+} is notably lower than the standard detection limit of 5 µM set by the World Health Organization (WHO) for Fe^{3+} in drinking water [17]. In this work, LODs for Fe^{2+} and $Fe^{3+}$are comparable to LODs reported by other sensors in the literature. The comparison results are presented in Table 2.

Table 2 Comparison of detection limits (LOD) and application of L sensor with other reported sensors for detection of Fe^{2+} and Fe^{3+} ions.

Metal ions	Solvent	LOD	Application	Reference
Fe^{2+}	H_2O-CH_3CN (v/v, 1/9)	7.4 µM	Biological samples	[18]
Fe^{2+}	DMSO	0.21 µM	Drinking water	[17]
Fe^{2+}	DMF	0.69 µM	Biological samples	[20]
Fe^{2+}	DMSO	0.32 µM	Biological samples	[19]
Fe^{2+}	THF-H_2O (v/v, 7/3)	0.6 µM	test strips	[16]
Fe^{2+}	DMSO-H_2O (v/v, 2/8)	0.45 µM	test strips	This work
Fe^{3+}	H_2O-CH_3CN (v/v, 1/9)	6.8 µM	Biological samples	[18]
Fe^{3+}	DMSO	0.19 µM	Drinking water	[17]
Fe^{3+}	DMF	0.44 µM	Biological samples	[20]
Fe^{3+}	ETOH-H_2O (v/v, 9/1)	5.16 µM	Drinking water	[27]
Fe^{3+}	DMSO	0.27 µM	Biological samples	[19]
Fe^{3+}	THF-H_2O (v/v, 7/3)	0.6 µM	test strips	[16]
Fe^{3+}	DMSO-H_2O (v/v, 2/8)	0.68 µM	test strips	This work

The Job plot method also known as the continuous variation method, is widely used for determining the binding stoichiometry of host-guest complexes. Initially, the solution of Schiff base macrocycle ligand sensor (L) and the solutions of Fe ions were prepared, after maintaining a consistent total concentration of solution, incremental amounts of Fe ions were separately added to the L sensor in a quartz cell (the cell was a total 1 mL volume). The molar ratio of the sensor (L) ([M]/[M] + [L]) was changed from 0 - 1 M. Afterward, the maximum absorbance intensity for Fe^{2+} and Fe^{3+} at their respective wavelengths was recorded [28]. The Job plot was constructed by plotting these recorded absorbances versus mole fraction of Fe^{2+} at 460 nm and Fe^{3+} at 456 nm (Figs. 10 and 11).

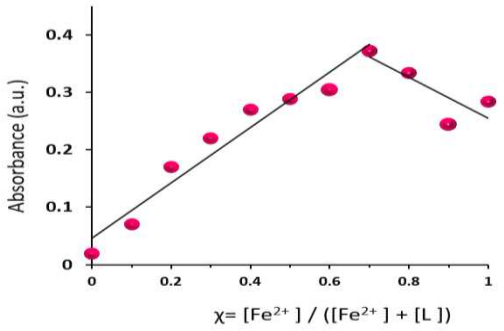

Fig. 10 Job's plot showing the 1:2 of L and Fe^{2+} under UV-Vis control (λ = 460 nm).

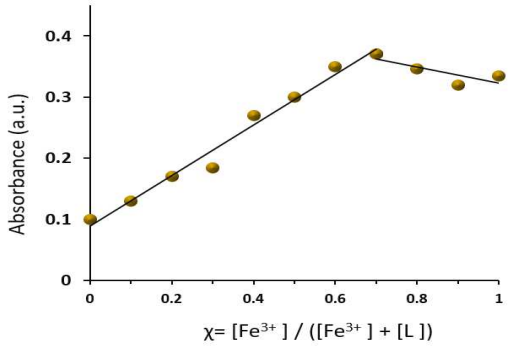

Fig. 11 Job's plot showing the 1:2 of L and Fe^{3+} under UV-Vis control (λ = 456 nm).

The binding stoichiometry between L and Fe ions was represented by the mole fraction of the complex at maximum absorption. According to the continuous changes in the mole fraction of Fe ions when the mole fraction of Fe ions was 0.66, the absorbance exhibited a maximum, demonstrating the 1:2 ratio of L: Fe ions (χ = 0.66), which confirms the formation of 1:2 complexes of ionic macrocycle Schiff base ligand (L) with Fe^{2+} and Fe^{3+} ions, separately [7,24].

3.7 Fluorescence experiments of L

3.7.1 The fluorescence studies of L for Fe^{2+} and Fe^{3+} responding

The fluorescence response of sensor L in DMSO: H_2O (2/8, v/v) solutions (5×10^{-5} M) were performed by adding various cations (Mo^{5+}, V^{4+}, Cr^{3+}, Al^{3+}, Zn^{2+}, Cd^{2+}, Hg^{2+}, Cu^{2+}, Ni^{2+}, Co^{2+}, Mn^{2+}, Sn^{2+}, Pb^{2+}, Fe^{3+}, Fe^{2+}, K^{+}, Ag^{+}, Mg^{2+}, Ca^{2+}, Ba^{2+}, Na^{+}) in equimolar concentrations (5×10^{-5} M) in DMSO: H_2O (2/8, v/v) solvent at room temperature (Fig. 12).The addition of different cations resulted in slight increases in the intensities of fluorescence emission bands. Interestingly, in the presence of Fe^{2+} and Fe^{3+} cations, the highest intensity is observed [21].

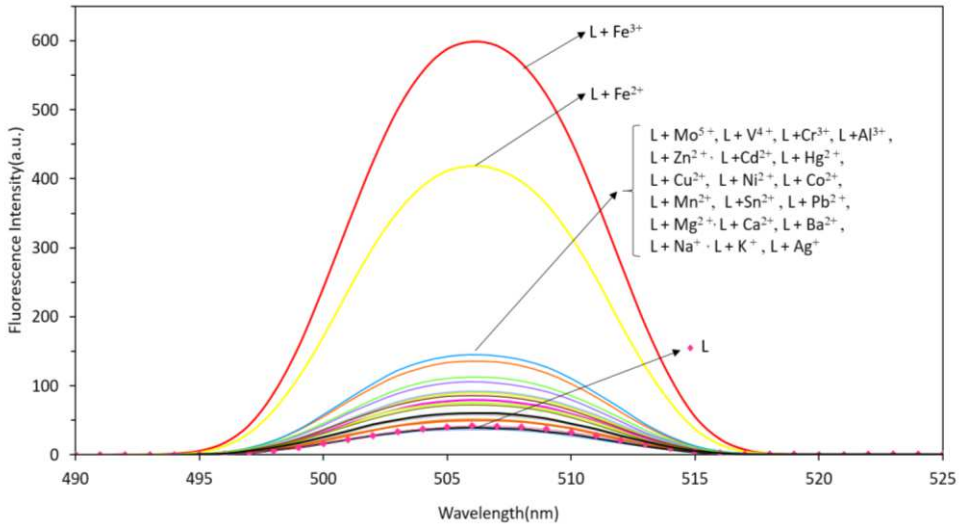

Fig. 12 Fluorescence spectra changes of L (5×10^{-5} M) after the addition of an equivalent amount of various cations at room temperature (λ_{max} = 506 nm) in DMSO: H_2O (2/8, v/v) λ_{ex} = 460 nm.

3.7.2 Fluorescence titration spectra

The sensitivity of L to Fe^{2+} and Fe^{3+} has also been confirmed through fluorescence titrations. As shown in Figs. 13 and 14, by gradually adding solutions of Fe^{2+} and Fe^{3+} at different concentrations (0-10 μM) in DMSO: H_2O (2/8, v/v) to a solution of L (5×10^{-5} M) in DMSO: H_2O (2/8, v/v), the fluorescence intensity of L increases without any shift in peak at λ_{max} = 506 nm and room temperature.

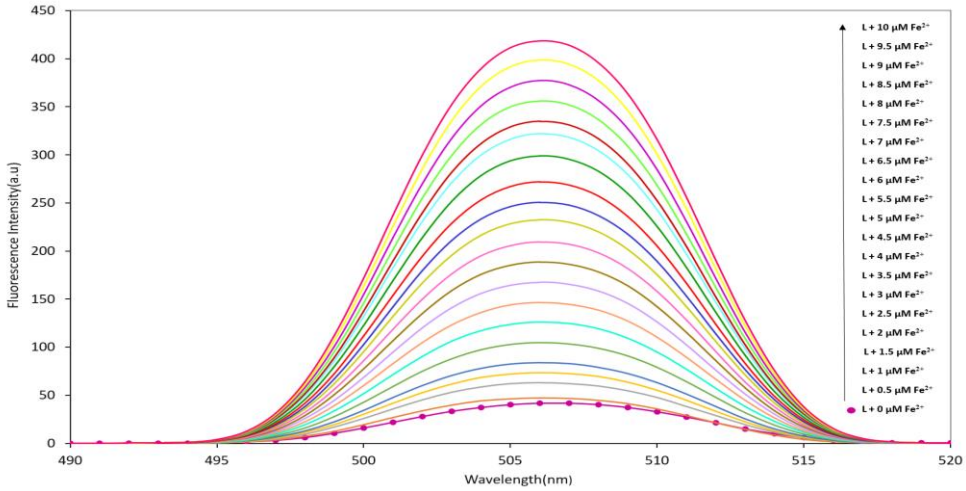

Fig. 13 Fluorescence emission spectra of L in DMSO: H_2O (2/8, v/v) solution (5×10^{-5}) upon gradual addition of Fe^{2+} (0 – 10 μM), (λ_{ex} = 460 nm, λ_{em} = 506 nm).

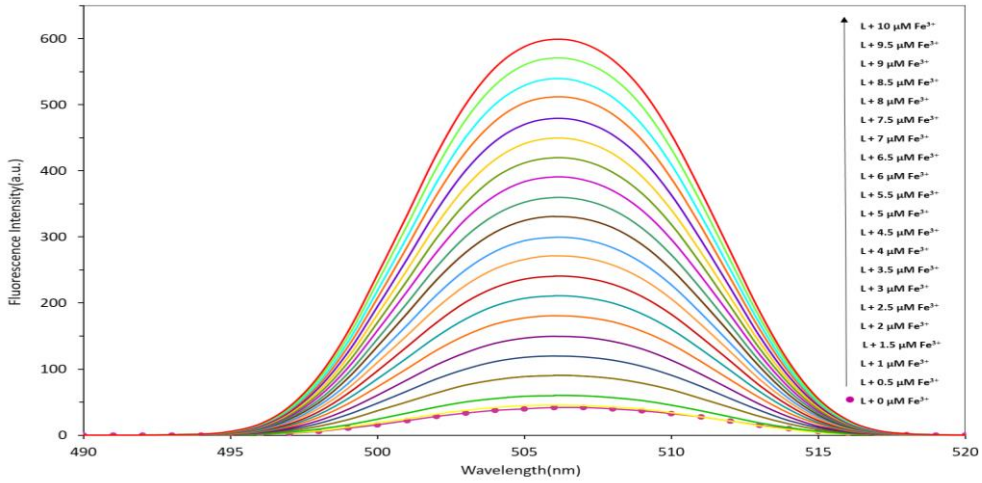

Fig. 14 Fluorescence emission spectra of L in DMSO: H_2O (2/8, v/v) solution (5×10^{-5}) upon gradual addition of Fe^{3+} (0 – 10 μM), (λ_{ex} = 456 nm, λ_{em} = 506 nm).

3.8 Proposed the sensing mechanisms of Fe^{2+} and Fe^{3+} cations by L

As discussed in previous sections, the addition of Fe^{2+} and Fe^{3+} cations to the sensor (L) causes rapid color changes in less than a second. In addition, in the UV-Vis spectrum of the sensor (L), significant changes occurred in the absorption bands upon the addition of Fe^{2+} and Fe^{3+} cations. The fluorescence emission bands of the sensor (L) have been significantly intensified by the addition of Fe^{2+} and Fe^{3+} cations. However, no significant changes were observed in the intensity of the emission bands of the L sensor in the presence of other tested cations. To evaluate the sensitivity and interaction of the sensor (L) with Fe^{2+} and Fe^{3+} cations, UV-Vis titrations and fluorescence emission titrations of the sensor (L) were performed by adding different concentrations (0-10 μM) of Fe^{2+} and Fe^{3+} ions separately. During these additions, the intensity of both absorption and emission bands also increased. This indicates the strong affinity of the sensor (L) to form complexes with Fe^{2+} and Fe^{3+} cations. Additionally, by using Job's diagram, the stoichiometric ratio of the sensor (L) to the Fe^{2+} cation in the L-Fe^{2+} complex was found to be 1:2. These results are similar to the stoichiometric ratio of L to the Fe^{3+} cation in the L-Fe^{3+} complex. When Fe^{2+} and Fe^{3+} cations are added to the sensor (L), they rapidly interact with the coordination sites in the L sensor compared to other tested cations. The binding results in the formation of L-Fe^{2+} and L-Fe^{3+} complexes have been

illustrated in Scheme 2. The ionic macrocycle Schiff base ligand sensor (L) binds to iron(II) and (III) ions by using oxygen atoms (OH) and imine nitrogen (C=N) in its structure forming a stable host-guest complex [7,22,40].

In addition, the UV-Vis spectrum of the L-Fe^{2+} and L-Fe^{3+} complexes shows a new absorption band at 460 nm and 358 nm for the L-Fe^{2+}, complex and 456 nm and 361 nm for the L-Fe^{3+} complex. These results confirm the proposed mechanism binding of the ionic macrocycle Schiff ligand sensor (L) to Fe^{2+} and Fe^{3+} cations, as well as the structures of L-Fe^{2+} and L-Fe^{3+} complexes [42].

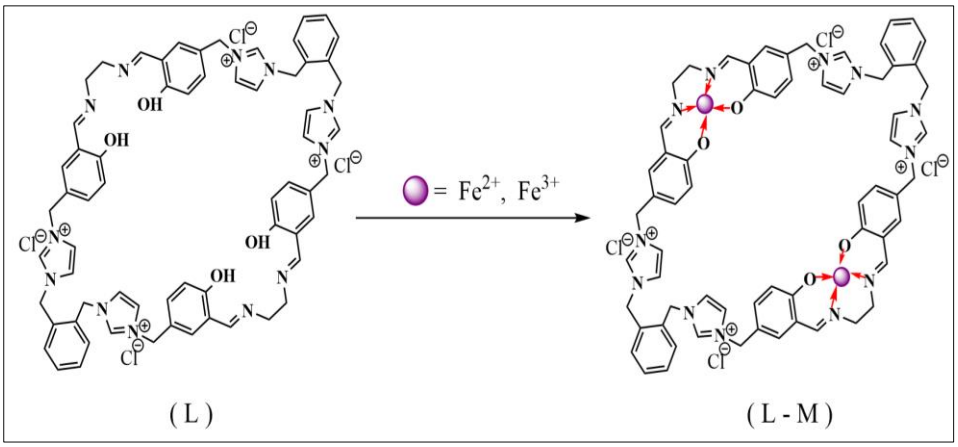

Scheme 2 Proposed sensing complexation mechanism of L with Fe^{2+} and Fe^{3+} ions.

The reversibility of L towards Fe^{2+} and Fe^{3+} was examined with ethylenediaminetetraacetic acid (EDTA) in DMSO: H_2O (2/8, v/v). As shown in Figs. 15 and 16, when EDTA (1 eq) was added to the L-Fe^{2+} and L-Fe^{3+} complexes, the solution color reverted to the original color of L. In addition, the absorbance at 460 nm and 456 nm disappeared immediately upon adding EDTA for L-Fe^{2+} and L-Fe^{3+} complexes, respectively. These results indicate the reversibility between the L-Fe^{2+} and L-Fe^{3+} complexes and EDTA [43].

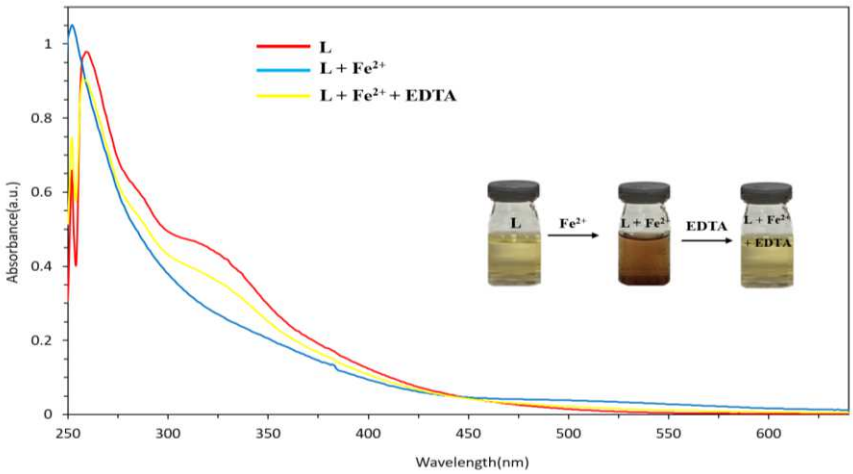

Fig. 15 UV-Vis spectral changes of L (5×10^{-5} M) after the addition of Fe^{+2} (5×10^{-5} M) and EDTA (1 eq) in DMSO: H_2O (2/8, v/v) solution.

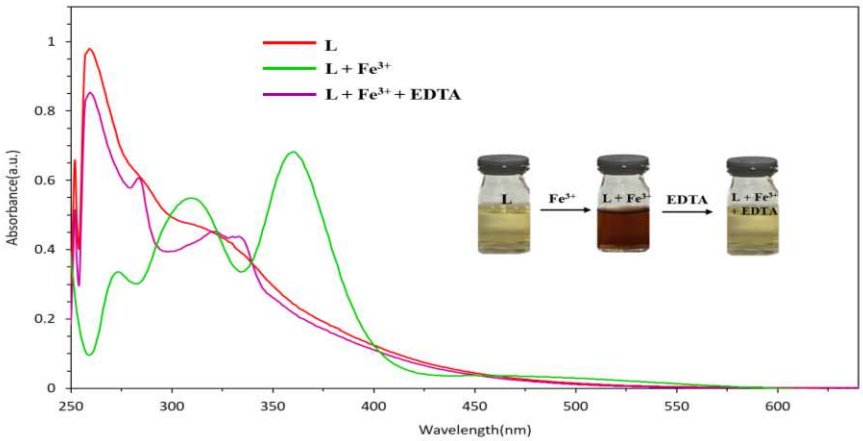

Fig. 16 UV-Vis spectral changes of L (5×10^{-5} M) after the addition of Fe^{+3} (5×10^{-5} M) and EDTA (1 eq) in DMSO: H_2O (2/8, v/v) solution.

3.9 The test paper strip

To detect Fe^{2+} and Fe^{3+} cations with L without complex tools, the colorimetric method using Whatman paper test strip sensors was investigated. Whatman papers were immersed in 10 ml of DMSO: H_2O solution (2/8, v/v) containing 3.7 mg (0.005 mmol) of L sensor for five seconds, then dried at room temperature. After immersing test strips covered with a sensor (L) in equimolar solutions of different metal cations (Mo^{5+}, V^{4+}, Cr^{3+}, Al^{3+}, Zn^{2+}, Cd^{2+}, Hg^{2+}, Cu^{2+}, Ni^{2+}, Co^{2+}, Mn^{2+}, Sn^{2+}, Pb^{2+}, Fe^{3+}, Fe^{2+}, K^+, Ag^+, Mg^{2+}, Ca^{2+}, Ba^{2+}, Na^+) in DMSO: H_2O solvent for five seconds, they were dried at room temperature. As observed in Fig. 17, the color of the test paper coated with the L sensor is gray in the absence of various cations but significant color changes were observed in the presence of Fe^{2+} and Fe^{3+} cations, from gray to brown-pale for Fe^{2+} and brownish yellow for Fe^{3+}, while the color changes caused by other metal cations are not significant. The paper kit method demonstrated that the ionic macrocycle Schiff base ligand (L) is highly sensitive and selective for detecting Fe^{2+} and Fe^{3+} cations respect to the other cations in real samples [44].

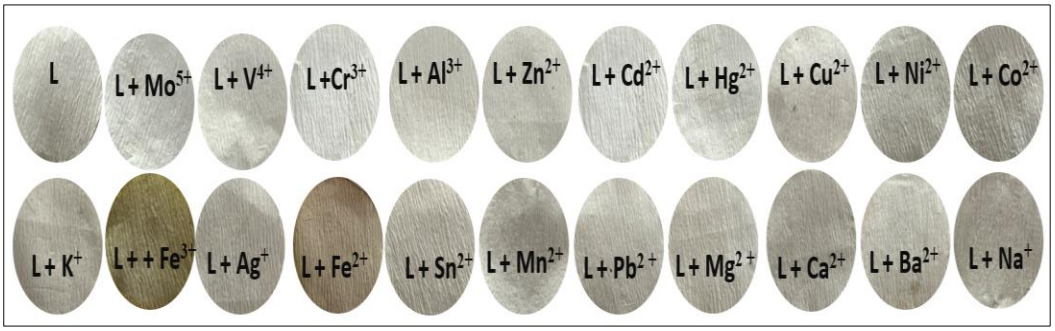

Fig. 17 The photographs of test strips after the addition of various cations under normal light at room temperature (left to right: L, Mo^{5+}, V^{4+}, Cr^{3+}, Al^{3+}, Zn^{2+}, Cd^{2+}, Hg^{2+}, Cu^{2+}, Ni^{2+}, Co^{2+}, K^+, Fe^{3+}, Ag^+, Fe^{2+}, Sn^{2+}, Mn^{2+}, Pb^{2+}, Mg^{2+}, Ca^{2+}, Ba^{2+} and Na^+).

4 Conclusions

In this work, a novel diimine two-tetradentate ionic macrocycle Schiff base ligand (L) has been synthesized and characterized by various analytical techniques such as FT- IR, ^{1}H NMR, ^{13}C NMR, LC-MS/MS spectrometry, etc. The cations recognition abilities by using L have been investigated by colorimetric assay. The L exhibited high selectivity and sensitivity for the detection of two metal cations Fe^{2+} and $Fe^{3+}$with color changes, respectively, from yellow to brown and brownish red, observable to the naked eye in aqueous media and at room temperature and in the presence of other cations. The possible recognition mechanism and the interaction between

the probe (L) for Fe^{2+} and Fe^{3+} were studied by UV-Vis titration, fluorescence titration, and Job curve. The LODs of L for Fe^{2+} and Fe^{3+} were calculated to be 0.45 μM and 0.68 μM, respectively. The binding stoichiometry ratio between host-guest (L and Fe ions) was 1:2, obtained from the Job plot. Also, the addition of EDTA indicated that L is a reversible sensor. Additionally, for the practical applicability of ligand as a sensor, test paper strip-based studies were done. These results divulge that the new diimine two-tetradentate ionic macrocycle Schiff base ligand (L) is useful as a colorimetric chemosensor for the detection of Fe^{2+} and Fe^{3+} by the naked eye.

Acknowledgments We are grateful to Damghan University (DU) for financial support.

References

[1] Zoubi, W.A., Al-Hamdani, A.A.S., Kaseem, M.: Synthesis and Antioxidant Activities of Schiff Bases and Their Complexes: A Review. Appl. Organomet. Chem. **30,** 810–817 (2016). https://doi.org/10.1002/aoc.3506.

[2] Ghanghas, P.; Choudhary, A.; Kumar, D.; Poonia, K.: Coordination Metal Complexes with Schiff Bases: Useful Pharmacophores with Comprehensive Biological Applications. Inorg. Chem. Commun. **130,** 108710 (2021). https://doi.org/10.1016/j.inoche.2021.108710.

[3] Wei, L., Zhang, J., Tan, W., Wang, G., Li, Q., Dong, F., Guo, Z.: Antifungal activity of double Schiff bases of chitosan derivatives bearing active halogeno-benzenes. Int. J. Biol. Macromol. **179**, 292-298 (2021). https://doi.org/10.1016/j.ijbiomac.2021.02.184

[4] Ommenya, F.K., Nyawade, E.A., Andala, D.M., Kinyua, J.: Synthesis, Characterization and Antibacterial Activity of Schiff Base, 4-Chloro-2-{(E)-[(4-Fluorophenyl)Imino]Methyl}phenol Metal (II) Complexes. J. Chem. **2020,** 1745236 (2020). https://doi.org/10.1155/2020/1745236.

[5] Bal, M., Köse, A.: Schiff bases containing 1, 2, 3-triazole group and phenanthroline: Synthesis, characterization, and investigation of DNA binding properties. J. Photochem. Photobiol. A. **448**. 115320 (2024). https://doi.org/10.1016/j.jphotochem.2023.115320.

[6] Ju, H., Chang, D.J., Kim, S., Ryu, H., Lee, E., Park, I.H., Jung, J.H., Ikeda, M., Habata, Y., Lee, S.S.: Cation-Selective and Anion-Controlled Fluorogenic Behaviors of a Benzothiazole-Attached Macrocycle That Correlate with Structural Coordination Modes. Inorg. Chem. **55**(15), 7448-7456 (2016). https://doi.org/10.1021/acs.inorgchem.6b00690.

[7] Alorabi, A.Q., Abdelbaset, M., Zabin, S.A.: Colorimetric Detection of Multiple Metal Ions Using Schiff Base 1-(2-Thiophenylimino)-4-(N-Dimethyl)Benzene. Chemosensors. **8**(1), 1 (2019). https://doi.org/10.3390/CHEMOSENSORS8010001.

[8] Khan, M.W., Mishra, R.P., Patel, B., Mishra, P., Vishwakarma, D.: Importance of Some Transition Metals and Their Biological Role: A Review, Int. Res. J. Pure Appl. Chem. **22**(5), 12-23 (2021). https://doi.org/10.9734/irjpac/2021/v22i530406.

[9] Wagner-Wysiecka, E., Łukasik, N., Biernat, J. F., Luboch, E.: Azo group (s) in selected macrocyclic compounds. J. Inclusion Phenom. Macrocyclic Chem. **90**, 189-257 (2018). DOI:10.1007/s10847-017-0779-4

[10] El-ghamry, M.A., Elzawawi, F.M., Aziz, A.A.A., Nassir, K.M., Abu-El-Wafa, S.M.: New Schiff Base Ligand and Its Novel Cr(III), Mn(II), Co(II), Ni(II), Cu(II), Zn(II) Complexes: Spectral Investigation, Biological Applications, and Semiconducting Properties. Sci. Rep. **12**, 17942 (2022). https://doi.org/10.1038/s41598-022-22713-z.

[11] Bougossa, I., Aggoun, D., Ourari, A., Berenguer, R., Bouacida, S., Morallon, E.: Synthesis and Characterization of a Novel Non-Symmetrical Bidentate Schiff Base Ligand and Its Ni(II) Complex: Electrochemical and Antioxidant Studies. Chem. Pap. **74**, 3825-3837 (2020). https://doi.org/10.1007/s11696-020-01200-7.

[12] Boulechfar, C., Ferkous, H., Delimi, A., Djedouani, A., Kahlouche, A., Boublia, A., Darwish, A.S., Lemaoui, T., Verma, R., Benguerba, Y.: Schiff Bases and Their Metal Complexes: A Review on the History, Synthesis, and Applications. Inorg. Chem. Commun. **150**, 110451 (2023). https://doi.org/10.1016/j.inoche.2023.110451.

[13] Li, Y., Niu, Q., Wei, T., Li, T.: Novel Thiophene-Based Colorimetric and Fluorescent Turn-on Sensor for Highly Sensitive and Selective Simultaneous Detection of Al^{3+} and Zn^{2+} in Water and Food Samples and Its Application in Bioimaging. Anal. Chim. Acta. **1049,** 196-212 (2019). https://doi.org/10.1016/j.aca.2018.10.043.

[14] Jothi, D., Munusamy, S., Sawminathan, S., Iyer, S.K.: Highly Sensitive Naphthalimide Based Schiff Base for the Fluorimetric Detection of Fe^{3+}. RSC Adv. **11**(19), 11338-11346 (2021). https://doi.org/10.1039/d1ra00345c.

[15] Oliveri, I.P., Attinà, A., Bella, S.D.: A Zinc (II) Schiff Base Complex as Fluorescent Chemosensor for the Selective and Sensitive Detection of Copper (II) in Aqueous Solution. Sensors. **23**(8) 3925 (2023). https://doi.org/10.3390/s23083925.

[16] Sasan, S., Chopra, T., Gupta, A., Tsering, D., Kapoor, K.K., Parkesh, R.: Fluorescence "Turn-Off" and Colorimetric Sensor for Fe^{2+}, Fe^{3+}, and Cu^{2+}Ions Based on a 2,5,7-Triarylimidazopyridine Scaffold. ACS Omega. **7**(13), 11114-11125 (2022). https://doi.org/10.1021/acsomega.1c07193.

[17] You, G.R., Park, G.J., Lee, S.A., Ryu, K.Y., Kim, C.: Chelate-type Schiff base acting as a colorimetric sensor for iron in aqueous solution, Sens. Actuators. B. **215**, 188-195 (2015). https://doi.org/10.1016/j.snb.2015.03.064.

[18] Choi, Y.W., Park, G.J., Na, Y.J., Jo, H.Y., Lee, S.A. , You, G.R., Kim, C.: A Single Schiff Base Molecule for Recognizing Multiple Metal Ions: A Fluorescence Sensor for Zn(II) and Al(III) and Colorimetric Sensor for Fe(II) and Fe(III). Sens. Actuators. B. **194**, 343-352 (2014). https://doi.org/10.1016/j.snb.2013.12.114.

[19] Jo, T.G. , BoK, K.H., Han, J., Lim, M.H., Kim. C.: Colorimetric detection of Fe^{3+} and Fe^{2+} and sequential fluorescent detection of Al^{3+} and pyrophosphate by an imidazole-based chemosensor in a near-perfect aqueous solution. Dyes Pigm. **139**, 136-147 (2017). https://doi.org/10.1016/j.dyepig.2016.11.052.

[20] Finelli, A., Chabert, V., Hérault, N., Crochet, A., Kim, C., Fromm, K.M.: Sequential multiple-target sensor: In^{3+}, Fe^{2+}, and Fe^{3+} discrimination by an anthracene-based probe. Inorg. Chem. **58**(20), 13796-13806 (2019). https://doi.org/10.1021/acs.inorgchem.9b01478.

[21] Soufeena, P.P., Aravindakshan, K.K.: Antipyrine Derived Schiff Base: A Colurimetric Sensor for Fe(III) and "Turn-on" Fluorescent Sensor for Al(III). J. Lumin. **205,** 400-405 (2019). https://doi.org/10.1016/j.jlumin.2018.09.025.

[22] Berhanu, A.L., Mohiuddin, I., Malik, A.K., Aulakh, J.S, Kumar, V., Kim, K.H.: A Review of the Applications of Schiff Bases as Optical Chemical Sensors. TrAC, Trends Anal. Chem. **116**, 74-91 (2019). https://doi.org/10.1016/j.trac.2019.04.025.

[23] Lestari, D., Wahyuningsih, T.D., Purwono, B.: Colorimetric Chemosensor for Sulfide Anion Detection Based on Symmetrical Nitrovanillin Azine, Indones. J. Chem. **23**(1), 12-20 (2023). https://doi.org/10.22146/ijc.71259.

[24] Zhang, P., Xu, X., Cui, Y.F., Wei, X.H., Sun, Y.X.: A Highly Sensitive and Selective Bissalamo-Coumarin-Based Fluorescent Chemical Sensor for Cr^{3+}/Al^{3+} Recognition and Continuous Recognition S^{2-}. J. Photochem. Photobiol. A. **408**, 113066 (2021). https://doi.org/10.1016/j.jphotochem.2020.113066.

[25] Özdemir, Ö.: Synthesis and Characterization of a New Diimine Schiff Base and Its Cu^{2+} and Fe^{3+} Complexes: Investigation of Their Photoluminescence, Conductance, Spectrophotometric and Sensor Behaviors. J. Mol. Struct. **1179**, 376-389 (2019). https://doi.org/10.1016/j.molstruc.2018.11.023.

[26] Sarkar, A., Chakraborty, A., Chakraborty, T., Purkait, S., Samanta, D., Maity, S., Das, D.: A Chemodosimetric Approach for Fluorimetric Detection of Hg^{2+} Ions by Trinuclear Zn(II)/Cd(II) Schiff Base Complex: First Case of Intermediate Trapping in a Chemodosimetric Approach. Inorg. Chem. **59**(13). 9014-9028 (2020). https://doi.org/10.1021/acs.inorgchem.0c00857.

[27] Alorabi, A.Q., Zabin, S.A., Alam, M.M. Abdelbaset, M.: Schiff Base Ligand 3-(-(2-Hydroxyphenylimino) Methyl)-4H-Chromen-4-One as Colorimetric Sensor for Detection of Cu^{2+}, Fe^{3+}, and V^{5+} in Aqueous Solutions. Int. J. Anal. Chem. **2022**(1), 4899145 (2022). https://doi.org/10.1155/2022/4899145.

[28] Tang, X., Han, J., Wang, Y., Ni, L., Bao, X., Wang, L., Zhang, W.: A Multifunctional Schiff Base as a Fluorescence Sensor for Fe^{3+} and Zn^{2+} Ions, and a Colorimetric Sensor for Cu^{2+} and Applications. Spectrochim. Acta, Part A. **173**, 721-726 (2017). https://doi.org/10.1016/j.saa.2016.10.028.

[29] Reyes.Márquez, V., Sánchez, M., Höpfl, H, Lara, K.O.: Synthesis and Structural Characterization of 18-, 19-, 20- and 22-Membered Schiff Base Macrocycles. J. Inclusion Phenom. Macrocyclic Chem. **65**, 305-315 (2009). https://doi.org/10.1007/s10847-009-9588-8.

[30] Lisowski, J.: Imine-and Amine-Type Macrocycles Derived from Chiral Diamines and Aromatic Dialdehydes. Molecules. **27**(13), 4097 (2022). https://doi.org/10.3390/molecules27134097.

[31] Hontz, D., Hensley, J., Hiryak, K., Lee, J., Luchetta, J., Torsiello, M., Venditto, M., Lucent, D., Terzaghi, W., Mencer, D., Bommareddy, A., VanWert, A.L.: A Copper(II) Macrocycle Complex for Sensing Biologically Relevant Organic Anions in a Competitive Fluorescence Assay: Oxalate Sensor or Urate Sensor?. ACS Omega. **5**(31), 19469-19477 (2020).https://doi.org/10.1021/acsomega.0c01655.

[32] Zhu, X., Duan, Y., Li, P., Fan, H., Han, T., Huang, X.: A Highly Selective and Instantaneously Responsive Schiff Base Fluorescent Sensor for the "Turn-off" Detection of Iron(III), Iron(II), and Copper(II) Ions. Anal. Methods. **11**(5), 642-647 (2019). https://doi.org/10.1039/c8ay02526f.

[33] Das, S., Aich, K., Goswami, S., Quah, C.K., Fun, H.K.: FRET-Based Fluorescence Ratiometric and Colorimetric Sensor to Discriminate Fe^{3+} from Fe^{2+}. New J. Chem. **40**(7), 6414-6420 (2016). https://doi.org/10.1039/c5nj03598h.

[34] El-Sonbati, A.Z., El-Bindary, A.A., Rashed, I.G.A.: Polymer Complexes XXXVII Novel Models and Structural of Symmetrical Poly-Schiff Base on Heterobinuclear Complexes of Dioxouranium(VI). Spectrochim. Acta, Part A. **58**(7), 1411-1424 (2002). https://doi.org/10.1016/S1386-1425(01)00592-3.

[35] Hoskins, B.F., Robson, R., Slizys, D.A.: An Infinite 2D Polyrotaxane Network in $Ag_2(Bix)_3(NO_3)_2$ (Bix = 1,4-Bis(Imidazol-1-Ylmethyl)Benzene). J. Am. Chem. Soc. **119**(12), 2952-2953 (1997). https://doi.org/10.1021/ja9642626.

[36] Sen, P., Akagunduz, D., Aghdam, A.S., Cebeci, F.Ç., Nyokong, T., Catal, T.: Synthesis of Novel Schiff Base Cobalt (II) and Iron (III) Complexes as Cathode Catalysts for Microbial Fuel Cell Applications. J. Inorg. Organomet. Polym. Mater. **30**, 1110-1120 (2020). https://doi.org/10.1007/s10904-019-01286-x.

[37] Golcu, A., Tumer, M., Demirelli, H., Wheatley, R.A.: Cd(II) and Cu(II) Complexes of Polydentate Schiff Base Ligands: Synthesis, Characterization, Properties and Biological Activity. Inorg. Chim. Acta. **358**(6), 1785-1797 (2005). https://doi.org/10.1016/j.ica.2004.11.026.

[38] Kedy, S., Almhna, N., Kandil, F.: Synthesis and Characterization of New Macrocyclic Schiff Bases by the Reaction of: 1,7-Bis (6-Methoxy-2-Formylphenyl)-1,7-Dioxaheptane and Their Use in Solvent Extraction of Metals. Arabian J. Chem. **8**(1), 93-99 (2015). https://doi.org/10.1016/j.arabjc.2011.01.013.

[39] Kianfar, M., Mohammadi, A.: A Simple and Sensitive Thiazole - Based Colorimetric Chemosensor for Detection of CN^-, AcO^- and Cu^{2+} Ions. J. Iran. Chem. Soc. **17,** 1429-1438 (2020). https://doi.org/10.1007/s13738-020-01867-5.

[40] Chae, J.B., Jang, H.J., Kim, C.: Sequential Detection of $Fe^{3+/2+}$ and Pyrophosphate by a Colorimetric Chemosensor in a near-Perfect Aqueous Solution. Photochem. Photobiol. Sci. **16,** 1812-1820 (2017). https://doi.org/10.1039/c7pp00354d.

[41] Jamal, H.S., Raja, R., Ahmed, S.W., Shah, M.R., Ahmed, S., Ali, S.A.: Simultaneous Colorimetric Sensing of Anion (I^-) and Cation (Fe^{2+}) by Protein Functionalized Silver Nanoparticles in Real Samples. J. Cluster Sci **33**(4), 1501-1514 (2022). https://doi.org/10.1007/s10876-021-02074-9.

[42] Yun, J.Y., Chae, J.B., Kim, M., Lim, M.H., Kim, C.: A Multiple Target Chemosensor for the Sequential Fluorescence Detection of Zn^{2+} and S^{2-} and the Colorimetric Detection of $Fe^{3+/2+}$ in Aqueous Media and Living Cells. Photochem. Photobiol. Sci. **18**, 166-176 (2019). https://doi.org/10.1039/c8pp00408k.

[43] Fernandes, R.S., Shetty, N.S., Mahesha, P., Gaonkar, S.L.: A comprehensive review on thiophene based chemosensors. J. Fluoresc. **32,** 19–56 (2022). https://doi.org/10.1007/s10895-021-02833-x.

[44] Kaur, M., Sahoo, S.C., Kaur, H.: New Schiff base as selective and sensitive detection of copper ions in aqueous solvent. ChemistrySelect. **5**, 14857-14868 (2020). https://doi.org/10.1002/slct.202003880

Supplementary Files

This is a list of supplementary files associated with this preprint. Click to download.

- SupplementaryInformationSITable.S1.docx